VIP Gas Separation Very Important Paper

International Edition: DOI: 10.1002/anie.201904507
German Edition: DOI: 10.1002/ange.201904507

A Metal–Organic Framework Based Methane Nano-trap for the Capture of Coal-Mine Methane

*Zheng Niu, Xili Cui, Tony Pham, Pui Ching Lan, Huabin Xing, Katherine A. Forrest, Lukasz Wojtas, Brian Space, and Shengqian Ma**

Abstract: *As a major greenhouse gas, methane, which is directly vented from the coal-mine to the atmosphere, has not yet drawn sufficient attention. To address this problem, we report a methane nano-trap that features oppositely adjacent open metal sites and dense alkyl groups in a metal–organic framework (MOF). The alkyl MOF-based methane nano-trap exhibits a record-high methane uptake and CH_4/N_2 selectivity at 298 K and 1 bar. The methane molecules trapped within the alkyl MOF were crystalographically identified by single-crystal X-ray diffraction experiments, which in combination with molecular simulation studies unveiled the methane adsorption mechanism within the MOF-based nano-trap. The IAST calculations and the breakthrough experiments revealed that the alkyl MOF-based methane nano-trap is a new benchmark for CH_4/N_2 separation, thereby providing a new perspective for capturing methane from coal-mine methane to recover fuel and reduce greenhouse gas emissions.*

Global warming, which is caused by the ever-increasing amount of greenhouse gases, is indisputably one of the most urgent and compelling problems this century.[1] As one of the major greenhouse gas, methane has significant effects as a greenhouse gas being 21 times higher than that of carbon dioxide, thereby causing serious environmental issues.[2] In recent years, about 29 to 41 billion cubic meters of methane have been liberated from underground coal mines, as coal-mine methane (CMM) every year, of which over 70% are directly vented to the atmosphere.[3] Further, the poor-quality CMM (methane content less than 50%, mainly balanced by nitrogen, usually at standard pressure) is difficult to be directly utilized.[4] Therefore, the separation of CH_4 from N_2 in poor-quality CMM could decrease the release of methane into the atmosphere while producing fuel gas concurrently, thereby generating significant economic and environmental benefits.

[*] Dr. Z. Niu, Dr. X. Cui, Dr. T. Pham, P. C. Lan, Dr. K. A. Forrest, Dr. L. Wojtas, Dr. B. Space, Dr. S. Ma
Department of Chemistry, University of South Florida
4202 E. Fowler Avenue, Tampa, FL 33620 (USA)
E-mail: sqma@usf.edu
Dr. X. Cui, Dr. H. Xing
Key Laboratory of Biomass Chemical Engineering of Ministry of Education, College of Chemical and Biological Engineering, Zhejiang University
Hangzhou 310027 (China)
Supporting information and the ORCID identification number(s) for the author(s) of this article can be found under: https://doi.org/10.1002/anie.201904507.

Compared with traditional cryogenic distillation, adsorbent-based gas separation methods, including pressure swing adsorption, temperature swing adsorption, and membranes, have been shown to be promising technologies to separate gases owing to their high energy efficiency and intrinsic economic feasibility.[5] However, the adsorptive separation of CH_4/N_2 mixtures has been found to be particularly difficult because of their similar kinetic diameters (3.8 Å for CH_4 and 3.6 Å for N_2) and comparable polarizability.[6] Traditional adsorbents of activated carbons and zeolites have been developed for CH_4/N_2 adsorptive separation, but they show a quite low separation selectivity and productivity,[7] thus urging the exploration of new types of adsorbents that can efficiently separate CH_4 from N_2.

As the emerging custom-designed porous materials, metal–organic frameworks (MOFs) show outstanding performance in gas separation owing to their tunable pore sizes and diverse functionalities.[8] In particular, the explicit single-crystal structure of MOF provides the opportunity to investigate the adsorption mechanism for specific gases, which can facilitate the design of new materials with better performance. Given the fact that CH_4 exhibits a slightly larger polarizability than N_2 (CH_4: 26.0×10^{-25} cm^3, N_2: 17.6×10^{-25} cm^3),[9] we reason that it is essential to increase the effective contact area or form multiple interactions to enhance the interaction between CH_4 molecules and the host framework for efficient CH_4/N_2 separation. Although some MOFs display excellent performance in high-pressure methane storage,[10] current top-performing MOFs exhibit low selectivity or low productivity for CH_4/N_2 separation at atmospheric pressure,[11] thus necessitating the development of new materials featuring stronger binding for capturing methane from CMM.

To achieve strong methane binding within a MOF, we contribute a new type of methane nano-trap that features oppositely adjacent coordinatively unsaturated metal centers and densely populated alkyl groups thus providing a methanephilic environment to trap methane molecules. Although it is known that coordinatively unsaturated metal centers can bind methane significantly, current MOFs with such open metal sites are ineffective in capturing methane at ambient/sub-ambient atmosphere owing to inadequate overlap of potential fields from opposite pore walls. As illustrated in Scheme 1, when two opposite coordinatively unsaturated metal centers are adjacent to each other, a nano-trap for methane can be generated based on the cooperative Coulombic interaction between the methane molecules and the two metal centers. In this regard, we chose an alkyl MOF, ATC-Cu, which features unique oppositely adjacent Cu-paddle wheel open metal sites and low polarity aliphatic

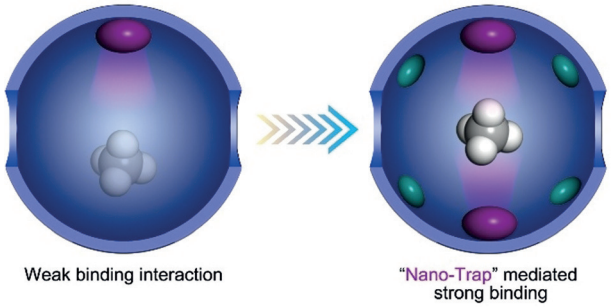

Scheme 1. The comparison of traditional methane adsorbent and nano-trap. The purple and green ellipsoids represent coordinatively unsaturated metal centers and alkyl groups, respectively.

hydrocarbon cavities, thereby increasing the energetic favorability toward methane molecules. Thanks to the methane nano-trap, the anhydrous ATC-Cu demonstrates the highest methane uptake amount at 1 bar among the reported MOFs, as well as the high CH_4/N_2 selectivity under such conditions.

The ATC-Cu (Cu_2(ATC)) is based on H_2ATC (1,3,5,7-adamantane tetracarboxylic acid) ligand and was synthesized through hydrothermal reaction.[12] As presented in Figure 1 a, the ATC ligand connects four Cu paddle-wheel secondary building units as a tetrahedral 4-coordinated linker to construct a 3D framework with rectangular channels (4.43 × 5.39 Å) along with *b* and *c* axes. The channel is constructed by the oppositely adjacent Cu-paddle wheels and aliphatic hydrocarbon cavities. The Cu–Cu distance between neighboring Cu paddlewheels is only 4.43 Å after subtracting van der Waals radius, thereby affording a considerable dual Coulombic interaction within this region and potentially generating a strong binding site for methane (Figure 1 b). Furthermore, there are twelve hydrogen atoms pointing toward the center of the aliphatic hydrocarbon cavities, and the average distance between these hydrogen atoms and center of the cavity is only 3.5 Å, which provides another potential adsorption site for methane (Figure 1 c). The

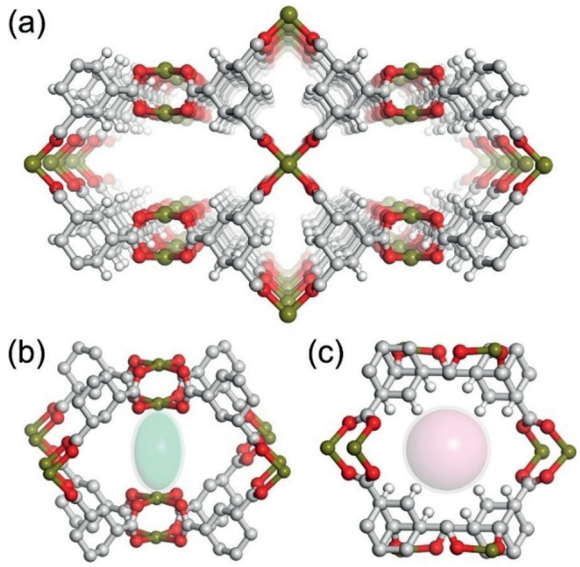

Figure 1. a) The channel of ATC-Cu. b) The adjacent Cu paddle-wheels in ATC-Cu. c) The aliphatic hydrocarbon cavity in ATC-Cu.

combination of aliphatic hydrocarbon low polarity cavities and the oppositely adjacent unsaturated metal sites endows ATC-Cu with the potential for high methane binding affinity. The N_2 sorption isotherm measurements of the activated ATC-Cu at 77 K indicates it has a Brunauer–Emmett–Teller surface area of 600 $m^2 g^{-1}$ and a total pore volume of 0.23 $cm^3 g^{-1}$.

The single-component adsorption isotherms for CH_4 and N_2 were collected for ATC-Cu at 273 K and 298 K (Figure 2 a). ATC-Cu was found to adsorb 2.90 mmol g^{-1} of CH_4 at 298 K and 1 bar, which exceeds that of all other reported high-performance CH_4 adsorbents. In contrast, the N_2 adsorption capacity of ATC-Cu is low, with an uptake amount of 0.75 mmol g^{-1} at 298 K and 1 bar. Furthermore, the value of

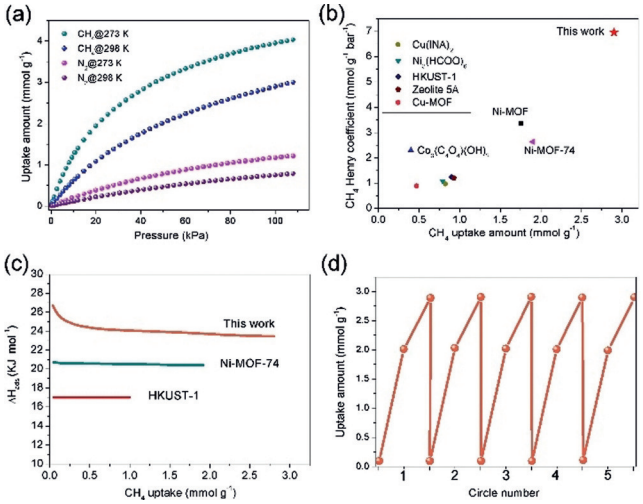

Figure 2. a) The methane and nitrogen adsorption isotherm for ATC-Cu at 273 and 298 K. b) CH_4 Henry coefficient plotted against uptake amount for high-performance methane adsorbents. c) The Q_{st} of CH_4 for high-performance MOFs with unsaturation metal sites. d) The recycle performance of ATC-Cu measured at 298 K and the testing pressure up to 1 bar without regeneration process.

the CH_4 Henry coefficient for ATC-Cu is the highest among reported methane adsorbent materials. As illustrated in Figure 2 b, ATC-Cu shows remarkable methane adsorption capability with both the highest uptake amount at 298 K/1 bar and the highest CH_4 Henry coefficient compared with current high-performance methane adsorbents (Supporting Information, Table S2) including zeolite-5A, $Co_3(C_4O_4)(OH)_2$, Cu-$(INA)_2$, $Ni_2(HCOO)_6$, HKUST-1, Ni-MOF-74, Cu-MOF, and Ni-MOF.[11]

The isosteric heats of adsorption (Q_{st}) of CH_4 and N_2 in the ATC-Cu were calculated using the dual-site Langmuir–Freundlich model to investigate the interaction strength between the gases and the framework (see the Supporting Information). As shown in Figure 2 c, the zero-coverage Q_{st} value for CH_4 in ATC-Cu (26.8 kJ mol^{-1}) is significantly higher than other high-performance MOFs, such as MOF-74-Ni (20.6 kJ mol^{-1}) and HKUST-1 (17.0 kJ mol^{-1}), implying an unusual strong binding interaction between methane and ATC-Cu. Compared with the methane, the Q_{st} value for N_2 in ATC-Cu is much lower (zero-coverage Q_{st} is 16.0 kJ mol^{-1} and

then slightly increased; Supporting Information, Figure S22), which shows a weak binding interaction. Furthermore, ATC-Cu exhibits excellent cycle performance in the CH_4 adsorption process (Figure 2d).

To understand the excellent methane adsorption performance of ATC-Cu, we conducted theoretical studies utilizing preliminary grand canonical Monte Carlo (GCMC) simulations and periodic density functional theory (DFT) calculations. ATC-Cu was found to exhibit two binding sites (site I and site II) for methane based on the calculation results. Site I is located in the middle of two oppositely adjacent Cu-paddle wheels, while site II is located in the aliphatic hydrocarbon cavity enclosed by four neighboring ATC linkers. As expected, the proximity of two unsaturated metal sites on oppositely neighboring Cu paddlewheels affords a methane nano-trap with enhanced Coulombic interaction, thereby generating a strong binding site for methane. A static adsorption energy was calculated to be 28.99 kJ mol^{-1} for site I, which confirms the strong interaction between the oppositely adjacent open metal sites and methane molecule. Compared with site I, the primary interaction for methane on site II is multiple van der Waals interactions with the nearby framework H atoms. There are twelve hydrogen atoms pointing toward the region that encompasses site II, which yields a relatively smaller static adsorption energy of 23.67 kJ mol^{-1} at this binding site according to the DFT calculations.

To further elucidate the strong binding affinity of ATC-Cu for methane, single-crystal X-ray diffraction (SCXRD) data was obtained for activated ATC-Cu crystals filled with methane (CH_4@ATC-Cu). As presented in Figure 3c and d, the methane molecule was located in the middle of the oppositely adjacent Cu-paddle wheels, consistent with the primary binding site (site I) determined by the modeling studies. The distance between the methane molecule and the adjacent open metal site (C–Cu) is 2.5 Å indicative of a strong interaction. Unfortunately, the methane molecule adsorbed within the aliphatic hydrocarbon cavity of ATC-Cu (site II) cannot be crystallographically identified under our in situ single-crystal X-ray diffraction experiment conditions, which would need higher pressures and lower temperatures to overcome the motion of methane molecules owing to the relatively weaker interaction. Nonetheless, the in situ single-crystal X-ray diffraction studies suggest that at atmospheric pressure and room temperature methane molecule can be well trapped by ATC-Cu through preferential binding to site I. The experimental zero-coverage Q_{st} (26.8 kJ mol^{-1}) is close to the static adsorption energy that was calculated about site I through periodic DFT calculations. The experimental gas adsorption data for ATC-Cu revealed that about two methane molecules were adsorbed in one unit cell of ATC-Cu at 1 bar and 298 K, which are primarily ascribed to the adsorption at site I.

Prompted by the large CH_4 Henry coefficient and the significant difference in Q_{st} between methane and N_2 in ATC-Cu (Supporting Information, Figures S21, S22), the CH_4/N_2 selectivity was calculated using ideal adsorbed solution theory (IAST) to evaluate the potential of ATC-Cu for capturing methane from mixtures that mimic CMM. As displayed in Figure 4a, the calculated CH_4/N_2 selectivity for the corresponding binary equimolar mixture in ATC-Cu is up to 9.7 at 298 K and 1 bar. The CH_4 uptake amount of ATC-Cu for a CH_4/N_2 equimolar mixture reaches 1.86 mmol g^{-1} at 298 K and 1 bar (Supporting Information, Figure S20), which is well above the current record (1.11 mmol g^{-1} for Ni-MOF[11e]). The IAST calculation revealed that the combination of the oppositely adjacent-open metal sites and alkane cavity can bestow a MOF material with both high productivity and high selectivity for methane from CH_4/N_2 gas mixtures.

To evaluate the CH_4/N_2 separation performance of ATC-Cu in potential industrial applications for capturing methane from CMM, experimental breakthrough experiments for CH_4/N_2 in different ratios (50/50, v/v; 30:70, v/v; 15/85, v/v)

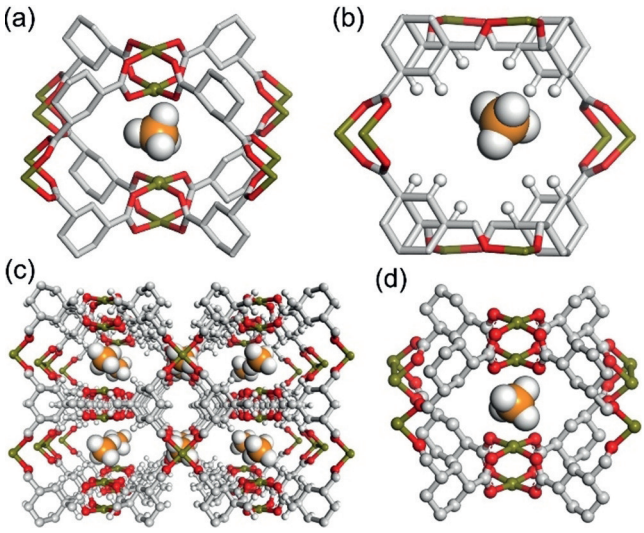

Figure 3. a) The binding site I between the adjacent Cu-metal sites and b) binding site II in the aliphatic hydrocarbon cavity of methane as determined by modeling studies conducted upon ATC-Cu. c) Single-crystal structure of methane loaded in ATC-Cu viewed along the *a* axis and d) close-up view.

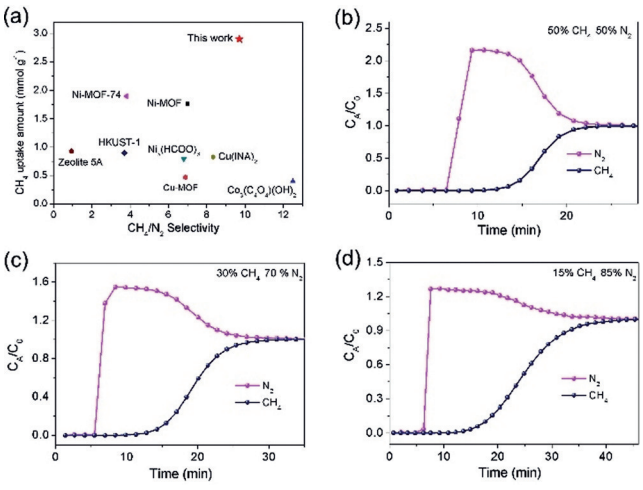

Figure 4. a) The CH_4/N_2 selectivity for high-performance materials at 1 bar and 298 K. b) IAST determined CH_4 uptake amount for an equimolar CH4/N2 mixture. c) Experimental column breakthrough curves for a 15:85 and 50:50 CH_4/N_2 mixture (298 K, 1 bar) in an adsorber bed packed with ATC-Cu.

at 298 K were conducted. The CH_4/N_2 mixture gases flowed over a packed column of activated ATC-Cu with a rate of 2 mL per min. For CH_4/N_2 (50/50, v/v) and CH_4/N_2 (30/70, v/v), complete separation of CH_4 from mixtures can be realized using activated ATC-Cu. Methane breakthrough occurred at 10.69 and 11.35 min for CH_4/N_2 (50/50 and 30/70 v/v), respectively. Notably, ATC-Cu shows great methane adsorption performance even in CH_4/N_2 (15/85, v/v), and the purity of CH_4 exceeds 99.99% before breakthrough occurring at 13.64 min. These results illustrate that ATC-Cu is a promising candidate for capturing methane from CMM with low content of methane at normal pressure and temperature.

In summary, we reported that a MOF-based methane nano-trap featuring unique oppositely adjacent open metal sites and aliphatic hydrocarbon cavities can induce strong interaction with methane, thereby affording outstanding methane adsorption and separation performance for potential use in capturing methane from CMM. The fundamental binding mechanism of ATC-Cu for methane has been illustrated through SCXRD studies and theoretical calculations, indicating this new type of MOF-based methane nano-trap can provide very strong binding sites for methane at relatively low pressure. The MOF-based methane nano-trap of ATC-Cu demonstrates a record high pure CH_4 uptake and CH_4 uptake in a binary equimolar CH_4/N_2 mixture at 298 K and 1 bar, making it a new benchmark material for the capture of methane from CMM. Our work not only provides a new approach to the development of porous materials with a strong binding affinity for methane to decrease the greenhouse gas emission, but also promotes MOFs with potential to resolve industrial challenges and environmental protection.

Acknowledgements

The authors acknowledge NSF (DMR-1352065) and the University of South Florida for financial support of this work. T.P., K.A.F., and B.S. acknowledge the support from NSF (DMR-1607989, CHE-1531590) and ACS Petroleum Research Fund (56673-ND6).

Conflict of interest

The authors declare no conflict of interest.

Keywords: coal-mine methane · cooperative effect · gas separation · metal–organic frameworks · nano-traps

How to cite: *Angew. Chem. Int. Ed.* **2019**, *58*, 10138–10141
Angew. Chem. **2019**, *131*, 10244–10247

[1] D. A. Lashof, D. R. Ahuja, *Nature* **1990**, *344*, 529–531.
[2] a) C. O. Karacan, F. A. Ruiz, M. Cote, S. Phipps, *Int. J. Coal Geol.* **2011**, *86*, 121–156; b) R. M. Flores, *Int. J. Coal Geol.* **1998**, *35*, 3–26.
[3] a) L. Sloss, Coalbed Methane Emissions: Capture and Utilisation. London: IEA Clean Coal Centre, **2005**; b) H. Limbri, C. Gunawan, B. Rosche, J. Scott, *Water Air Soil Pollut.* **2013**, *224*, 1566.
[4] a) T. L. Saleman, G. Li, T. E. Rufford, P. L. Stanwix, K. I. Chan, S. H. Huang, E. F. May, *Chem. Eng. J.* **2015**, *281*, 739–748; b) C. M. Liu, Y. P. Zhou, Y. Sun, W. Su, L. Zhou, *AIChE J.* **2011**, *57*, 645–654.
[5] D. S. Sholl, R. P. Lively, *Nature* **2016**, *532*, 435–437.
[6] J. R. Li, R. J. Kuppler, H. C. Zhou, *Chem. Soc. Rev.* **2009**, *38*, 1477–1504.
[7] a) K. V. Kumar, F. Rodriguez-Reinoso, *Nanotechnology* **2013**, *24*, 035401; b) B. Majumdar, S. J. Bhadra, R. P. Marathe, S. Farooq, *Ind. Eng. Chem. Res.* **2011**, *50*, 3021–3034.
[8] a) R. B. Lin, S. C. Xiang, H. B. Xing, W. Zhou, B. L. Chen, *Coord. Chem. Rev.* **2019**, *378*, 87–103; b) J. M. Yu, L. H. Xie, J. R. Li, Y. G. Ma, J. M. Seminario, P. B. Balbuena, *Chem. Rev.* **2017**, *117*, 9674–9754; c) K. Adil, Y. Belmabkhout, R. S. Pillai, A. Cadiau, P. M. Bhatt, A. H. Assen, G. Maurin, M. Eddaoudi, *Chem. Soc. Rev.* **2017**, *46*, 3402–3430; d) Q. G. Zhai, X. H. Bu, X. Zhao, D. S. Li, P. Y. Feng, *Acc. Chem. Res.* **2017**, *50*, 407–417; e) D. Banerjee, A. J. Cairns, J. Liu, R. K. Motkuri, S. K. Nune, C. A. Fernandez, R. Krishna, D. M. Strachan, P. K. Thallapally, *Acc. Chem. Res.* **2015**, *48*, 211–219; f) Q. Y. Yang, D. H. Liu, C. L. Zhong, J. R. Li, *Chem. Rev.* **2013**, *113*, 8261–8323; g) J. R. Li, J. Sculley, H. C. Zhou, *Chem. Rev.* **2012**, *112*, 869–932; h) J. R. Li, Y. G. Ma, M. C. McCarthy, J. Sculley, J. M. Yu, H. K. Jeong, P. B. Balbuena, H. C. Zhou, *Coord. Chem. Rev.* **2011**, *255*, 1791–1823; i) Y. Wang, N.-Y. Huang, X.-W. Zhang, H. He, R.-K. Huang, Z.-M. Ye, Y. Li, D.-D. Zhou, P.-Q. Liao, X.-M. Chen, J.-P. Zhang, *Angew. Chem. Int. Ed.* **2019**, https://doi.org/10.1002/anie.201902209; *Angew. Chem.* **2019**, https://doi.org/10.1002/ange.201902209; j) J. E. Bachman, M. T. Kapelewski, D. A. Reed, M. I. Gonzalez, J. R. Long, *J. Am. Chem. Soc.* **2017**, *139*, 15363–15370; k) H.-G. Hao, Y.-F. Zhao, D.-M. Chen, J.-M. Yu, K. Tan, S. Ma, Y. Chabal, Z.-M. Zhang, J.-M. Dou, Z.-H. Xiao, G. Day, H.-C. Zhou, T.-B. Lu, *Angew. Chem. Int. Ed.* **2018**, *57*, 16067–16071; *Angew. Chem.* **2018**, *130*, 16299–16303; l) L. Li, H.-M. Wen, C. He, R.-B. Lin, R. Krishna, H. Wu, W. Zhou, J. Li, B. Li, B. Chen, *Angew. Chem. Int. Ed.* **2018**, *57*, 15183–15188; *Angew. Chem.* **2018**, *130*, 15403–15408; m) Y.-L. Peng, T. Pham, P. Li, T. Wang, Y. Chen, K.-J. Chen, K. A. Forrest, B. Space, P. Cheng, M. J. Zaworotko, Z. Zhang, *Angew. Chem. Int. Ed.* **2018**, *57*, 10971–10975; *Angew. Chem.* **2018**, *130*, 11137–11141; n) Y. Wang, W. Liu, Z. Bai, T. Zheng, M. A. Silver, Y. Li, Y. Wang, X. Wang, J. Diwu, Z. Chai, S. Wang, *Angew. Chem. Int. Ed.* **2018**, *57*, 5783–5787; *Angew. Chem.* **2018**, *130*, 5885–5889; o) Z. Bao, J. Wang, Z. Zhang, H. Xing, Q. Yang, Y. Yang, H. Wu, R. Krishna, W. Zhou, B. Chen, Q. Ren, *Angew. Chem. Int. Ed.* **2018**, *57*, 16020–16025; *Angew. Chem.* **2018**, *130*, 16252–16257.
[9] R. T. Yang, *Adsorbents: Fundamentals and Applications*, Wiley, Hoboken, **2003**.
[10] Y. Peng, V. Krungleviciute, I. Eryazici, J. T. Hupp, O. K. Farha, T. Yildirim, *J. Am. Chem. Soc.* **2013**, *135*, 11887–11894.
[11] a) L. Li, L. Yang, J. Wang, Z. Zhang, Q. Yang, Y. Yang, Q. Ren, Z. Bao, *AIChE J.* **2018**, *64*, 3681–3689; b) X. F. Wu, B. Yuan, Z. B. Bao, S. G. Deng, *J. Colloid Interface Sci.* **2014**, *430*, 78–84; c) J. Hu, T. Sun, X. Liu, Y. Guo, S. Wang, *RSC Adv.* **2016**, *6*, 64039–64046; d) Y. Guo, J. L. Hu, X. W. Liu, T. J. Sun, S. S. Zhao, S. D. Wang, *Chem. Eng. J.* **2017**, *327*, 564–572; e) C. E. Kivi, B. S. Gelfand, H. Dureckova, H. T. K. Ho, C. Ma, G. K. H. Shimizu, T. K. Woo, D. Song, *Chem. Commun.* **2018**, *54*, 14104–14107; f) D. Saha, Z. Bao, F. Jia, S. Deng, *Environ. Sci. Technol.* **2010**, *44*, 1820–1826.
[12] B. Chen, M. Eddaoudi, T. M. Reineke, J. W. Kampf, M. O'Keeffe, O. M. Yaghi, *J. Am. Chem. Soc.* **2000**, *122*, 11559–11560.

Manuscript received: April 11, 2019
Version of record online: May 22, 2019

